Proceedings Paper:

Colombo, M. orcid.org/0000-0002-4335-4250, De Santis, A., Hanson, B.C. et al. (1 more author) (2021) A novel generalized multifluid modelling approach for the simulation of multiphase flows: model development and validation. In: Hickel, S., Salvetti, M.V. and Rodi, W., (eds.) Proceedings of the 13th International ERCOFTAC Symposium. 13th International ERCOFTAC Symposium on Engineering Turbulence Modelling and Measurements (ETMM 13), 15-17 Sep 2021, Rhodes, Greece. ERCOFTAC , pp. 88-93.

A Novel Generalized Multifluid Modelling Approach for the Simulation of Multiphase Flows: Model Development and Validation

M. Colombo, A. De Santis, B.C. Hanson, M. Fairweather

School of Chemical and Process Engineering, University of Leeds, Leeds LS2 9JT, United Kingdom

M.Colombo@leeds.ac.uk

Abstract

Multiphase gas-liquid flows exist in a large variety of flow regimes with interfaces that often span over a broad range of length scales. This paper introduces the generalized multifluid modelling approach (GEMMA), developed to predict the complex multiphase regimes where dispersed and large scale interfaces co-exist. The GEMMA solver introduces interface resolving capabilities inside a multifluid framework, by selectively applying a dispersed or a large interface multifluid formulation based on the local interfacial scale. Validation of the model against fundamental segregated and dispersed flow conditions is achieved. These include a rising bubble in liquid at rest, where the model achieves an accuracy comparable to interface resolving techniques, a stratified laminar flow and a bubbly pipe flow, where the model operates in the dispersed regime. In the final part, the solver is used to predict a stratified turbulent flow, where modelling of the turbulence at the interface is mandatory for the accurate prediction of the phase velocities and distribution.

1 Introduction

Multiphase flows are ubiquitous in nature and in a wide range of engineering applications and industrial processes and equipment. The unlimited variety of multiphase flows found in practical applications differs not only because of the number and type of the phases involved (solid, liquid, gas), but also due to many possible spatial arrangements of these phases in the multiphase flow field. To different arrangements correspond different morphologies of the interface, and specific impacts on the flow behaviour and the transport of mass, momentum and energy across the interface. Due to this large variety, multiphase flows have been historically classified in different flow regimes (e.g., bubbly flow, slug flow, annular flow) as a function of the phase arrangement.

Overall, gas-liquid and liquid-liquid multiphase flows can be distinguished into dispersed regimes, where a large number of small-scale bubbles or droplets are dispersed in a continuous fluid region. On the other hand, in segregated or stratified flows large scale interfaces form from the agglomeration of droplets or bubbles into larger structures like slugs, or due to the action of gravity. Unfortunately, such distinctive features are not often found in large scale flows that are of industrial interest. Instead, multiple flow regimes co-exist and interact with each other and interface structures span a wide range of length scales depending on the local flow conditions (e.g., bubbles can coalesce into large continuous gas structures and entrainment of bubbles/droplets into continuous liquid/gas regions can occur due to the perturbation of the interface in separated flows). When this is coupled to the complex, large scale geometry of many industrial turbulent flows the resulting system becomes, even for the most advanced computational models, an almost unsolvable, truly multiscale problem.

Even with computational fluid dynamics (CFD), successful results have been obtained only for specific flow conditions, and general applicability to multiple regimes remains a major issue. Dispersed regimes have been successfully modelled using multifluid Eulerian-Eulerian models. In these, the interface is not resolved but filtered in the averaging procedure, and all the interfacial transfers are modelled with closure relations (Liao et al., 2018; Colombo et al., 2021). However, multifluid models tend to diffuse large interfaces and their averaged formulation is not equipped to handle large, intermittent interface structures that extend over multiple mesh elements (Bestion, 2014).

Instead, with interface resolving techniques, all the interface scales are entirely resolved and the models have successfully been employed to resolve segregated regimes and large interfaces (Mehrabani et al., 2017; Zimmer and Bolotnov, 2019). However, their application to dispersed regimes is constrained by computational costs to fundamental flows with a limited number of droplets or bubbles.

Recently, attempts have been made, mainly by implementing interface resolving capabilities in multifluid solvers, to develop a generalized methodology that is not limited to specific flow regimes (Strubelj et al., 2009; Hänsch et al., 2013). Most of these implementations rely, in the presence of large interfaces, on compression algorithms, designed to counteract the numerical diffusion unavoidably affecting multifluid models (Gada et al., 2017; Mathur et al., 2019). In conjunction to this, a dedicated closure framework is activated, normally including a large interface drag closure and a model for the surface tension force.

This work presents a generalized multifluid modelling approach (GEMMA) (De Santis et al., 2021), applicable to n-phases and developed starting from the *reactingMultiphaseEulerFoam* solver of the OpenFOAM CFD code (The OpenFOAM Foundation, 2016). The model is sensitive to the local flow morphology and interface compression, and switching between dispersed and large interfaces is activated based on the local gradient of the void fraction or the dispersed phase to the computational grid size ratio, avoiding the arbitrary void fraction thresholds used in the majority of these models (Hänsch et al., 2013; Gada et al., 2017; Mathur et al., 2019). In addition, blending between dispersed and segregated closure frameworks is achieved in a generalized way that is applicable to any interfacial closure without modification. Here, validation of the model against fundamental segregated and dispersed cases is presented. These include the rising of a bubble in a stagnant liquid, a stratified laminar flow and a dispersed bubbly flow. Finally, application to a stratified flow (Fabre et al., 1987), relevant for the study of loss of coolant accidents in nuclear thermal hydraulics, is also presented. Applications of the model to other more complex cases including liquid-liquid extraction processes are presented in a companion paper at this conference.

2 GEMMA concept

The GEMMA solver is developed on top of the Eulerian-Eulerian multifluid *reactingMultiphaseEulerFoam* solver of OpenFOAM (The OpenFOAM Foundation, 2016), where a set of conservation equations is solved for n compressible phases. While this work is limited to adiabatic flows, mass, momentum, energy and species conservation equations can be solved. The general form of the conservation equations for a multifluid model is presented in numerous available publications (Prosperetti and Tryggvason, 2007; Yeoh and Tu, 2010). In the GEMMA solver, a numerical compressive term is added to the continuity equation, to counteract numerical diffusion and maintain a sharp interface in segregated regimes (Wardle and Weller, 2013):

$$\frac{\partial}{\partial t}(\alpha_k\rho_k) + \nabla\cdot(\alpha_k\rho_k\boldsymbol{u}_k) + \nabla \cdot [\alpha_k(1-\alpha_k)\rho_k\boldsymbol{u}_c] = 0 \tag{1}$$

The artificial compression velocity $\boldsymbol{u}_c$ is obtained from the local relative velocity and the interface normal vector, which ensures it acts perpendicular to the interface:

$$\boldsymbol{u}_c = C_\alpha|\boldsymbol{u}_r|\frac{\nabla\alpha}{|\nabla\alpha|} \tag{2}$$

Here, C_α is a scalar field that is equal to 0 when the flow is dispersed and 1 in segregated regions with large interfaces. Therefore, it is through C_α that GEMMA distinguishes between the multifluid formulation in dispersed regimes and the multifluid interface-resolving formulation with large interfaces. Following the work of Wardle and Weller (2013), the large interface mode is activated locally when a sufficient mesh resolution is achieved. This is defined through a local Interface Resolution Quality (IRQ) that needs to be higher than a critical value:

$$IRQ = \frac{2}{\Delta\kappa} > IRQ_{crit} \tag{3}$$

where Δ is the local mesh size and κ the interface curvature. The value of the IRQ increases for more refined resolution of the interface. Therefore, the critical value identifies a minimum resolution that needs to be reached for the large interface model to be activated. If this requirement is met, the large interface mode is effectively activated if the local void fraction gradient is higher than a certain value (identifying the presence of a large interface) or, when GEMMA is coupled to a population balance model, the local length scale of the dispersed phase is larger than the grid spacing by at least a factor Γ:

$$d_{SM} > \Gamma\Delta \tag{4}$$

In Eq. (4), d_{SM} is the Sauter-mean diameter. In addition to the compression in Eq. (1), GEMMA adapts the multifluid model to the local interface morphology, by selectively changing the multifluid closure framework. In the momentum equation, the dynamic interaction between the phases is modelled with a series of forces, each of which accounts for a different mechanism of interfacial momentum transfer:

$$\boldsymbol{M}_k = \boldsymbol{F}_d + \boldsymbol{F}_l + \boldsymbol{F}_w + \boldsymbol{F}_{td} + \boldsymbol{F}_{vm} + \boldsymbol{F}_{st} \tag{5}$$

Eq. (5) includes drag, lift, wall lubrication, turbulent dispersion, virtual mass and surface tension forces, and $\boldsymbol{M}_k$ is the interfacial transfer term in the momentum equation of phase k. In the dispersed regime, all the forces except for surface tension can be included. Instead, in the large interface mode, only drag, modelled with a large interface closure, and surface tension remain active. This is achieved by coupling the native volume fraction based blending function already implemented in OpenFOAM with the C_α field. The GEMMA drag force closure for the entire range of regimes has the following form:

$$\boldsymbol{F}_d = [1-(1-C_\alpha)f_{gl}-(1-C_\alpha)f_{lg}]\boldsymbol{F}_{d,LI} + (1-C_\alpha)f_{gl}\boldsymbol{F}_{d,gl} + (1-C_\alpha)f_{lg}\boldsymbol{F}_{d,lg} \tag{6}$$

In the previous equation, $\boldsymbol{F}_{d,LI}$ is the large interface drag closure, which provides the drag force when $C_\alpha = 1$. $\boldsymbol{F}_{d,gl}$ and $\boldsymbol{F}_{d,lg}$ are the drag closures for gas in liquid and liquid in gas, and f_{gl} and f_{lg} the OpenFOAM native blending functions, with linear and hyperbolic options available. For lift, wall lubrication, turbulent dispersion and virtual mass the formulation is similar, except that they are equal to zero in the large interface mode. Surface tension, instead, is active only with large interfaces:

$$\boldsymbol{F}_{st} = C_\alpha \boldsymbol{F}_{st,LI} \tag{7}$$

Information on the specific closures used for each case test below is provided in the results section. Although limited here to interface momentum transfer, the updated GEMMA blending method is already applicable with no restrictions to any interfacial closure.

When required, turbulence is modelled using a mixture k-ε model (Behzadi et al., 2004), to avoid the numerical instabilities related to resolving a specific phase turbulence in regions where its volume fraction is negligible. In the mixture dissipation ε_m equation, a specific dissipation source is included, to avoid unphysical turbulence kinetic energy values near large interfaces. The model is taken from Frederix et al. (2018) and adapted to the mixture formulation:

$$S_{\varepsilon,m} = C_\alpha \left[\sum_{k=l,g} C_2 \alpha_k \rho_k \left(\frac{\nu_k}{\delta^2} \right)^2 k_k \right] \tag{8}$$

In Eq. (8), ν_k is the kinematic viscosity of phase k and δ a parameter equal to 10^{-4}.

3 Results and discussion

A first validation of the model was made against the case of a bubble rising in a stagnant liquid, often used in the validation of multiphase models given the availability of benchmark solutions from three different interface capturing codes (Hysing et al., 2009). The setup is a two-dimensional 1 × 2 m (width × height) liquid domain, where a 0.5 m bubble is suspended 0.5 m above the bottom of the liquid at the beginning of the simulation. Fluid properties and computational settings were taken from Hysing et al. (2009). The Eötvös and Morton number are 9.0 and 6 × 10^{-4}, which correspond to bubbles of ellipsoidal shape in the well-known Grace diagram (Grace et al., 1976). The simulation was run for ~ 3 s, with a time-step size adjusted to maintain the Courant number below 0.25. In this assessment, we are interested in the capability of GEMMA to identify the interface of the bubble and maintain a sharp interface while it rises towards the top of the tank. For this reason, only the drag and the surface tension are considered in the momentum interfacial closure. The drag models of Marschall (2011) and Ishii and Zuber (1979) are employed in the large interface and dispersed model, and the surface tension is modelled following De Santis et al. (2021) and it is active only with large interfaces.

In Figure 1, snapshots of the rising bubble at 0.0, 1.5 and 3.0 s are provided. The first and the third images display the gas volume fraction, showing how the bubble, which is spherical at the start, rises and assumes an ellipsoidal shape, a result of the correct modelling of the interfacial forces involved. At 1.5 s, instead, the C_α field is displayed. This shows how the large interface is properly detected by GEMMA, allowing the interface to remain sharp in the simulation. Also in Figure 1, the bubble average velocity as a function of time is displayed. GEMMA agrees well against the benchmark solution and the volume of fluid method, except for a slight underprediction of the rising velocity in the first second, probably as a consequence of an overestimated interfacial drag.

The second test is a laminar stratified flow in a horizontal channel of 0.02 m height. The two dimensional channel is 0.04 m long and it is modelled with an imposed pressure gradient, no-slip walls on top and bottom and zero gradient conditions at the inlet and outlet. The flow is initialized as stratified with the interface in the middle of the channel. The two fluids have the same density but different viscosity, equal to 1.85 × 10^{-5} for the fluid on the bottom and 5 × 10^{-4} for the fluid on the top.

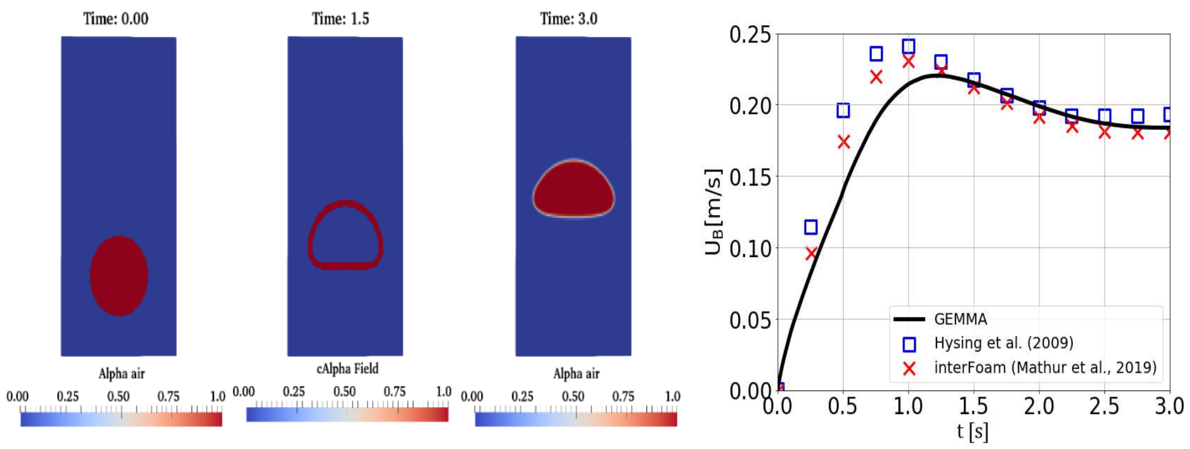

Figure 1: Simulation of the rising bubble test case from Hysing et al. (2009). On the left, the void fraction, and the C_α fields are shown. On the right, the bubble rising velocity is compared against Hysing et al. (2009) and an interFoam simulation (from Mathur et al. (2019)).

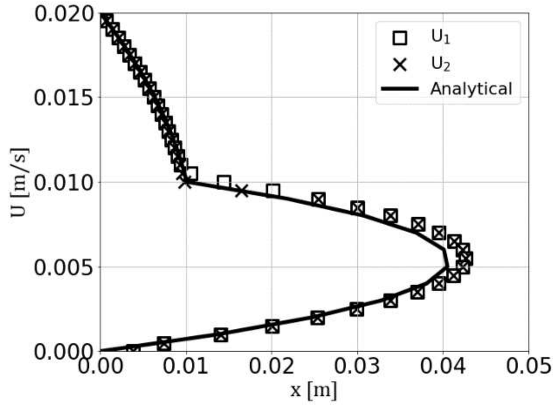

Figure 2: Velocity profile for a laminar stratified flow with two fluids with the same density but different viscosities compared against an analytical solution.

The behaviour of the multiphase flow is effectively governed by the interfacial drag. Therefore, as in the previous case, only dispersed and large interface drag and the surface tension are modelled. An analytical solution is available for this case, which has been used by other authors for the validation of their hybrid multifluid approaches (Marschall, 2011; Mathur et al., 2019). In Figure 2, the vertical velocity profile taken in the middle of the channel is shown. The velocity profile in both fluids is well predicted, as is the velocity difference at the interface. The latter is a clear indication of a correct prediction of the drag in the region of the large interface.

The previous two cases were focused on assessing the behaviour of GEMMA in the large interface regime. Now, instead, the model operation in a dispersed flow is assessed by simulating a turbulent upward bubbly flow in vertical pipe. The test is taken from the air-water experiments of Hosokawa and Tomiyama (2009) in a 25 mm inner diameter pipe. Specifically, the experiment at liquid superficial velocity j_l = 1.0 ms^{-1} and gas superficial velocity j_g = 0.036 ms^{-1} is selected. The bubble diameter is fixed in the entire domain at 3.66 mm, equal to the average bubble diameter measured in the experiment. The void fraction is 0.033, positioning the case in the low-void, dispersed bubbly flow regime. The computational domain corresponds to a quarter section of the pipe, with no-slip imposed at the wall, uniform velocity and void fraction fixed at the inlet and pressure fixed in the outlet section. On the lateral sides, symmetry boundary condition is imposed.

In this pipe flow, the model is expected to operate in the dispersed regime, and the full interfacial momentum closure framework is necessary to correctly predict the behaviour of the bubble. Drag (Ishii and Zuber, 1979), lift (Tomiyama et al., 2002), wall (Antal et al., 1991) and turbulent dispersion force (Burns et al., 2004) are all considered in the dispersed regime. If large interfaces were to be detected, large interface drag and surface tension will be activated to model the dynamic interaction at the interface.

The air distribution inside the pipe, and a radial profile of the void fraction compared against experimental measurements are displayed in Figure 3. The void distribution shows the characteristic wall-peaked profiles where bubbles, which have a close to spherical shape, are pushed toward the wall by the lift force. Hydrodynamic effects at the wall then prevent the bubbles from moving closer, causing the peak observed in the experiment. GEMMA results demonstrate that the model operates in the dispersed regime. While the main features of the void accumulation and the peak value reached are in good agreement with the experiments, the shape of the peak is not reproduced, probably as a consequence of a too weak wall force.

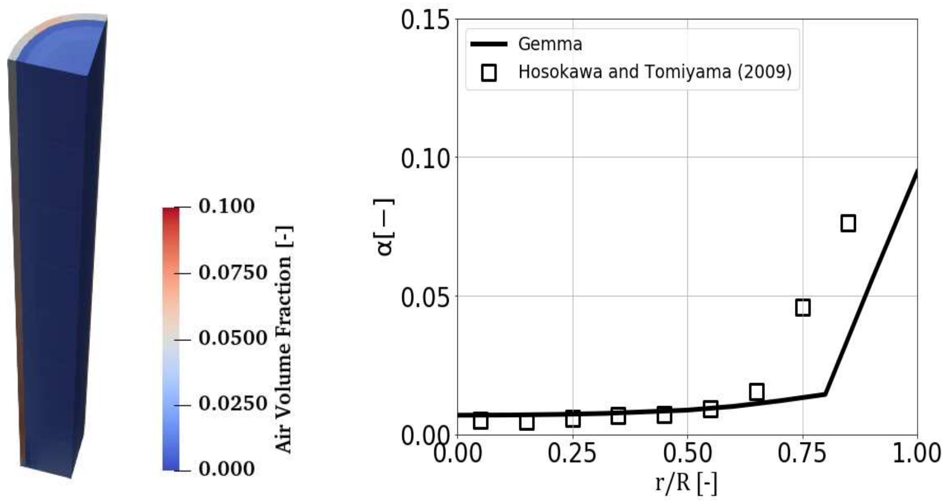

Figure 3: Simulation results of a bubbly vertical pipe flow experiment from Hosokawa and Tomiyama (2009) (Case 4). Void fraction field (left) and comparison against experimental data for the radial void profile (right).

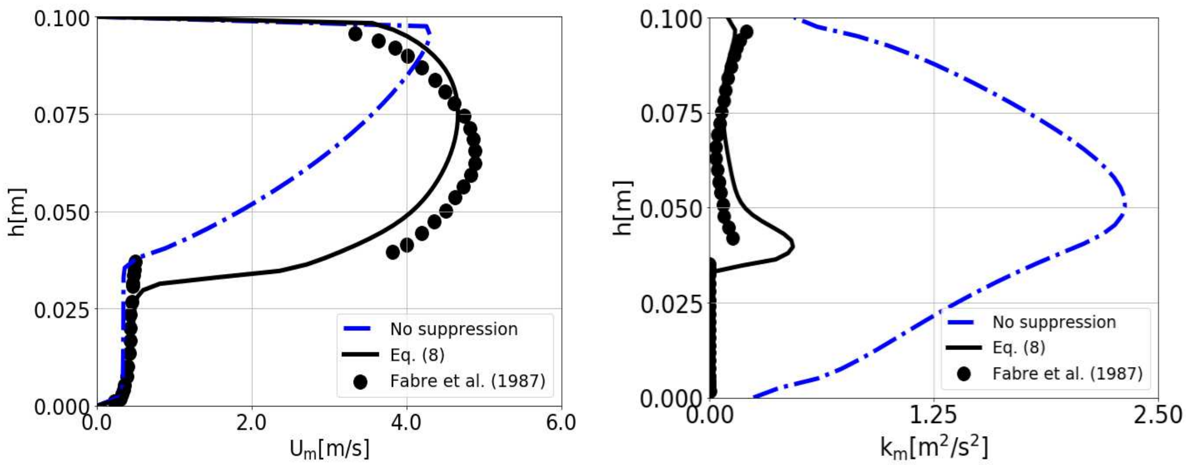

Figure 4: Mixture velocity (left) and turbulence kinetic energy (right) as a function of the height in the channel with and without interface turbulence suppression.

Although the accuracy of the model could have been further improved by a different selection of the interfacial force closures, this was outside the scope of the present work which was instead focused on the applicability of the GEMMA solver across multiple flow regimes.

Finally, the model is applied to a co-current stratified flow of air and water in the rectangular channel studied by Fabre et al. (1987). A 10 × 0.1 m two dimensional model of the channel is set up, with results recorded at 9.1 m from the inlet as in the experiment. In the experiment, water and air are injected with volumetric flow rates 3.0 ls^{-1} for the water and 45.4 ls^{-1} for the air and a smooth stratification was observed without any entrainment reported. In the simulation, the liquid level is fixed at the inlet equal to the measured value of 0.038 m, and uniform velocities of water and air are imposed to match the flow rates in the experiment. The no-slip condition is imposed on the upper and lower wall and pressure is instead fixed on the outlet section. After a sensitivity study, a 3000 × 60 node computational grid was found sufficient to obtain grid independent solutions. Given that a stratified flow is expected, only drag and surface tension are again considered, while lift, wall and turbulent dispersion forces are neglected. The turbulence is modelled with a mixture k-ε model, with the specific source of dissipation in Eq. (**8**) included.

A stable, stratified flow was also achieved in the simulation, with only minor observed perturbations of the large interface, which was correctly detected by the model, causing the activation of the large interface regime. In view of this, results were averaged over 30 s for comparison against experiments. Mean velocity and turbulence kinetic energy profiles along the channel height are displayed in Figure 4. Agreement with experiment is obtained only by including suppression of the turbulence at the interface, in the absence of which turbulence is largely overestimated. The high level of turbulence, which corresponds a very high value of turbulent viscosity, introduces excessive resistance to the flow in the interfacial region, forcing the gas to favour the upper portion of the channel, where a pronounced peak is displayed near the upper wall. Instead, with turbulence suppression, the correct parabolic profile is recovered and results are in good agreement with experiments. In the plot, the mixture velocity is shown, which corresponds to the gas velocity over the interface, and to the liquid velocity under the interface. The same is true for the turbulence kinetic energy, which is also in very good agreement with experiments in the bulk of the flow when suppression is included. The discrepancies still present near the interface, where turbulence is still slightly overpredicted on the gas side and shows a near zero value on the liquid side, is worth further investigation.

4 Conclusions

The generalized multifluid model GEMMA has been developed and implemented in conjunction with the multifluid *reactingMultiphaseEulerFoam* solver. Interface sharpening inside the multifluid framework is achieved by means of an interface compression algorithm that is dynamically activated locally in the presence of large interfaces. The model was successfully validated against test cases where a sharp interface needs to be maintained such as a rising bubble and a laminar stratified flow. Comparison against a bubbly pipe flow demonstrated the capabilities of the model in the dispersed regime, where compression is not activated and a dispersed set of interfacial closures is used. A more complex turbulence stratified flow is also well-predicted, when turbulence suppression in the interface region is included in the turbulence model. More complex applications including liquid-liquid extraction processes are the subject of a companion paper at this conference.

Acknowledgements

This work was undertaken on ARC4, part of the High Performance Computing facilities at the University of Leeds. MC acknowledges the support of the EPSRC through grant EP/S019871/1 "Towards comprehensive multiphase flow modelling for nuclear reactor thermal hydraulics". ADS and BH acknowledge the support of the EU project GENIORS (Project ID: 755171) on "GEN IV Integrated Oxide Fuels Recycling Strategies" and of the UK Department for Business, Energy and Industrial Strategy's through the Advanced Fuel Cycle Programme.

References

Antal, S.P., Lahey, R.T. and Flaherty, J.E. (1991), Analysis of phase distribution in fully developed laminar bubbly two-phase flow, *Int. J. Multiphase Flow*, Vol. 17, pp. 635-652.

Behzadi, A., Issa, R.I. and Rusche, H. (2004), Modelling of dispersed bubble and droplet flow at high phase fractions, *Chem. Eng. Sci.*, Vol. 59, pp. 759-770.

Bestion, D. (2014), The difficult challenge of a two-phase CFD modelling for all flow regimes, *Nucl. Eng. Des.*, Vol. 279, pp. 116-125.

Burns, A.D., Frank, T., Hamill, I. and Shi, J.M. (2004), The Favre averaged drag model for turbulent dispersion in Eulerian multi-phase flows, 5th International Conference on Multiphase Flows, Yokohama, Japan, May 30 - June 4.

Colombo, M., Rzehak, R., Fairweather, M., Liao, Y. and Lucas, D. (2021), Benchmarking of computational fluid dynamic models for bubbly flows, *Nucl. Eng. Des.*, Vol. 375, 111075.

De Santis, A., Colombo, M., Hanson, B.C. and Fairweather, M. (2021), A generalized multiphase modelling approach for multiscale flows, *J. Comput. Phys.*, Vol. 436, 110321.

Fabre, J., Masbernat, L. and Suzanne, C. (1987), Experimental data set no. 7: stratified flow, part I: local structure, *Multipahse Sci. Technol.*, Vol. 3, pp. 285-301.

Frederix, E.M.A., Mathur, A., Dovizio, D., Geurts, B.J. and Komen, E.M.J. (2018), Reynolds-averaged modelling of turbulence damping near a large-scale interface in two-phase flow, *Nucl. Eng. Des.*, Vol. 333, pp. 122-130.

Gada, V.H., Tandon, M.P., Elias, J., Vikulov, R. and Lo, S. (2017), A large scale interfacial multi-fluid model for simulating multiphase flows, *Appl. Math. Model.*, Vol. 44, pp. 189-204.

Grace, J.R., Wairegi, T. and Nguyen, T.H. (1976), Shapes and velocities of single drops and bubbles moving freely through immiscible liquids, *T. Inst. Chem. Eng.*, Vol. 54, pp. 167-173.

Hänsch, S., Lucas, D., Krepper, E. and Hohne, T. (2013), A multi-field two-fluid concept for transitions between different scales of interfacial structures, *Int. J. Multiphase Flow*, Vol. 47, pp. 171-182.

Hosokawa, S. and Tomiyama, A. (2009), Multi-fluid simulation of turbulent bubbly pipe flow, *Chem. Eng. Sci.*, Vol. 64, pp. 5308-5318.

Hysing, S., Turek, S., Kuzmin, D., Parolini, N., Burman, E., Ganesan, S. and Tobiska, L. (2009), Quantitative benchmark computations of two-dimensional bubble dynamics, *Int. J. Numer. Meth. Fl.*, Vol. 60, pp. 1259-1288.

Ishii, M. and Zuber, N. (1979), Drag coefficient and relative velocity in bubbly, droplet or particulate flows, *AIChE J.*, Vol. 25, pp. 843-855.

Liao, Y., Ma, T., Liu, L., Ziegenhein, T., Krepper, E. and Lucas, D. (2018), Eulerian modelling of turbulent bubbly flow based on a baseline closure concept, *Nucl. Eng. Des.*, Vol. 337, pp. 450-459.

Marschall, H. (2011), Towards numerical simulation of multi-scale two-phase flows, PhD Thesis, Technische Universitat Munchen

Mathur, A., Dovizio, D., Frederix, E.M.A. and Komen, E.M.J. (2019), A Hybrid Dispersed-Large Interface Solver for multi-scale two-phase flow modelling, *Nucl. Eng. Des.*, Vol. 344, pp. 69-82.

Mehrabani, M.T., Nobari, M.R.H. and Tryggvason, G. (2017), An efficient front-tracking method for simulation of multi-density bubbles, *Int. J. Numer. Meth. Fl.*, Vol. 84, pp. 445-465.

Prosperetti, A. and Tryggvason, G. (2007), Computational methods for multiphase flow, Cambridge University Press, Cambridge, United Kingdom.

Strubelj, L., Tiselj, I. and Mavko, B. (2009), Simulations of free surface flows with implementation of surface tension and interface sharpening in the two-fluid model, *Int. J. Heat Fluid Fl.*, Vol. 30, pp. 741-750.

The OpenFOAM Foundation (2016), OpenFOAM v7 User Guide.

Tomiyama, A., Tamai, H., Zun, I. and Hosokawa, S. (2002), Transverse migration of single bubbles in simple shear flows, *Chem. Eng. Sci.*, Vol. 57, pp. 1849-1858.

Wardle, K.E. and Weller, H.G. (2013), Hybrid multiphase CFD solver for coupled dispersed/segregated flows in liquid-liquid extraction, *Int. J. Chem. Eng.*, Vol. 2013, 128936.

Yeoh, G.H. and Tu, J.Y. (2010), Computational techniques for multiphase flows - Basics and applications, Butterworth-Heinemann, Elsevier, Oxford, United Kingdom.

Zimmer, M.D. and Bolotnov, I.A. (2019), Slug-to-churn vertical two-phase flow regime transition study using an interface tracking approach, *Int. J. Multiphase Flow*, Vol. 115, pp. 196-206.